

BIOMEDICAL PARAMETER MEASUREMENTS USING
VIDEO PROCESSING

by

NEGAR ZIAEE NASRABADI

Presented to the Faculty of the Graduate School of
The University of Texas at Arlington in Partial Fulfillment
of the Requirements
for the Degree of

MASTER OF SCIENCE IN COMPUTER SCIENCE

THE UNIVERSITY OF TEXAS AT ARLINGTON

MAY 2015

Copyright © by NEGAR ZIAEE NASRABADI 2015

All Rights Reserved



Acknowledgements

I would like to express my sincere gratitude to my advisor, Associate Professor Manfred Huber, who has been extremely supportive through this study. I appreciate his crucial advice, knowledge, and clear-sighted discussion in conducting and finalizing my thesis. Without his help this thesis would not have been accomplished. I am also very grateful to my thesis committee, Doctor Farhad Kamangar, and Doctor David Levine, for their supportive advice, time and concern.

Sincere thanks to John Haroutunian, who spent his time in discussing and reviewing this thesis. I also would like to thank you Oluwatosin Oluwadare for his support. This experiment would have not been able to be completed without his help.

I cannot thank enough to my parents for supporting me throughout all my studies at the university.

April 20, 2015

Abstract

BIOMEDICAL PARAMETER MONITORING USING VIDEO PROCESSING

Negar Ziaee Nasrabadi, M.S.

The University of Texas at Arlington, 2015

Supervising Professor: Manfred Huber

For quite some time, patients' cardiovascular parameters have been measured by sensors connected to their body. One way of measuring these parameters is pulse oximetry by using an optical technique. It uses a photodetector to detect light absorption changes of red and infrared light. These two types of light serve as two sources of illumination. These current types of methods for monitoring parameters are often viewed as uncomfortable by the patient, and therefore are not desirable for frequent and long periods of monitoring. Furthermore, these methods can potentially produce a psychologically influenced bias from the patient because the patient is physically involved with the monitoring. As a result, there is a desire for a more patient friendly method for measuring cardiovascular parameters.

Recent research has shown that the cardiovascular parameters can be measured by using a camera's digital video of a person's face and daylight as an illumination source. This research opens a vast opportunity for remote, low cost, and convenient monitoring of cardiovascular parameters. Using the optical technique, these novel methods extract the cardiovascular signal using light reflected from the face, and it ultimately allows important data about the cardiovascular parameters to be extracted from a distance. These parameters include the blood flow signal, heart rate, blood

oxygen, and blood pressure. Furthermore, these methods allow frequent and remote monitoring of a patient in a given environment while also guaranteeing that the parameters obtained are free from patient bias. As a result, this method can routinely measure the patient's parameters during long periods of time which is desirable.

This line of research has been extended in this research by designing a system to measure the changes of blood related health conditions more conveniently. The low cost system analyzes the whole face and processes the reflected light signal of a local area on the face. In this study we use visible and infrared light as a source of illumination to measure the parameters using different light spectrum wavelengths which include red, green, and infrared light.

The method investigated here is advantageous because the patients' comfort level is not sacrificed for accurate monitoring, and because it allows for routine and long term monitoring. Routine monitoring of the cardiovascular parameters' changes is desired because the parameters that are influenced by illness are frequently tracked. Ultimately, it allows the monitoring and tracking of the illness' progression and thus supports a more accurate diagnosis than traditional techniques.

Table of Contents

Acknowledgements	iii
Abstract	iv
List of Illustrations	viii
List of Tables	ix
Chapter 1 Introduction.....	1
1.1 Objective.....	1
1.2 Outline	2
Chapter 2 Related Work.....	3
2.1 Eulerian Video Magnification	3
2.2 Heart Rate Estimation Using Smart Phone Camera	4
2.3 Heart Rate Estimation Using Video Camera	6
Chapter 3 Background	11
3.1 Photoplethysmography.....	11
3.2 Pulse Wave and PPG signal	14
3.3 Infrared wavelength	15
3.4 Signal Processing	16
3.4.1 Face Recognition.....	17
3.4.2 Face Feature Extraction	18
3.4.3 KLT Point Tracking algorithm	19
3.4.4 Temporal filtering.....	20
3.5 Heart Rate Variability.....	20
Chapter 4 Technical.....	22
4.1 Environment.....	23
4.2 Region of Interest Detection and Tracking	23

4.3 PPG Signal Filtering	26
4.4 Heart rate	28
Chapter 5 Conclusion and Future Work.....	37
References	39
Biographical Information	44

List of Illustrations

Figure 3-1 The ECG Signal and Equivalent PPG Pulse Signal [4].....	11
Figure 3-2 Main tissue absorption spectrum. [39].....	12
Figure 3-3 Proper red and infrared light wavelength to read PPG signal [27].....	13
Figure 3-4 Volume and pressure shape and features [14]	15
Figure 3-5 Water (H ₂ O), Oxygenated hemoglobin (HbO ₂), and Deoxygenated hemoglobin (Hb) light absorption spectrum in the near-infrared range [27]	16
Figure 4-1 Face recognition, feature extraction	24
Figure 4-2 Selected Features and ROI	25
Figure 4-3 Left Cheek ROI original and filtered signal.....	26
Figure 4-4 Right ROI original and filtered signal.....	27
Figure 4-5 Forehead Cheek ROI original and filtered signal	27
Figure 4-6 Frequency analysis of the PPG signal and the output heart rate signal. The mean heart rate is 65.45 bpm	30
Figure 4-7 Frequency analysis of the PPG signal and the output heart rate signal. The mean heart rate is 78.88 bpm	31
Figure 4-8 an example of sharper filtered signal, the corresponding autocorrelation results, the extracted HRV, and the distribution for the same HRV signal.	36

List of Tables

Table 4-1 the result of the signal extracted from a 120 fps video from a light skin subject. The most accurate mean heart rate and the standard deviation are shown in red.	32
Table 4-2 the result of signal extracted from a 120 fps video from a dark skin subject. The most accurate mean heart rate and the standard deviation are shown in red.....	34

Chapter 1

Introduction

Monitoring of vital signs such as heart rate and blood pressure on a regular basis is important to early detect illnesses and the onset of chronic health conditions as well as for the effective treatment and management of illnesses. For preventive and diagnostic purposes it is thereby desirable that this monitoring occurs free of the white coat effect, which leads to elevated readings if measurements are taken in the presence of a medical professional or under psychological stress situations. As a result, methods that can take these measurements in the home and with minimal involvement of the individual would be ideal as they ensure both the absence of psychological bias in the measurements and the collection of the information at regular intervals and over long periods of time. A combination of image and advanced digital signal processing can be used to achieve this and to monitor the vital signs of a person, such as the heart rate and blood flow using a video captured by a qualified camera. This technique, in contrast to previously used techniques such as pulse oximetry, can be autonomous and occur largely without the active involvement of the individual. The advantages of autonomous cardiovascular measurement are that it is more convenient, can obtain readings more frequently and on a more regular basis, and that it is less affected by user error. However, autonomous visual techniques have a need for a controlled setting in order to ensure reliable measurements, requiring supporting actions such as light control and that the user looks straight at a camera for a limited period of time without major movement.

1.1 Objective

The objective of thesis is to develop and evaluate methods for a smart mirror to extract the blood related vital health parameters, such as blood flow and heart rate. This will facilitate more frequent health monitoring of a person's parameters in their residential

environment, providing potentially useful diagnostic information to a doctor, or allowing the system to inform emergency services in the event of a critical health condition.

This work involves extracting vital signs from a sequence of video frames by detecting the changes of reflected light from the face and analyzing the signal to measure the blood flow and heart rate. The experiment performed uses visible and infrared light as a source of illumination and shows the viability of the approach for health monitoring.

1.2 Outline

This section contains a brief overview of the chapters of this thesis.

Chapter 1 provides a concise introduction to the problem that addressed in this thesis discusses the importance of this problem, introduces our proposed solution to this problem.

Chapter 2 is a brief review of related work that has been already performed for similar problems, their implemented solutions that have been introduced and implemented to solve the problem, and the results that were obtained.

Chapter 3 defines and describes the underlying concepts and algorithms that have been used to implement the solution. In addition, discusses the details of the experiment.

Chapter 4 presents the solution proposed in this thesis in detail and introduces the details of how it was implemented. It also presents the experiment that was performed and discusses its environmental setup. As part of this experiment, it provides a comparison of different experiment factors and environments, and finally the experimental results and an assessment of the reliability of the introduced method.

Chapter 2

Related Work

This chapter reviews the current frameworks and technologies that have been introduced and implemented for noninvasive measuring of vital sign parameters. These technologies focus on optical methods which attempt to extract these parameters from a signal extracted from video or other optical recording captured from a face or finger by a video camera or a phone camera. These parameters include blood flow, mean heart rate, and respiratory rate.

2.1 Eulerian Video Magnification

Eulerian video magnification [1] is one of the novel methods to reveal and measure the blood flow in the face. This method visualizes the blood flow in the face and small head motions caused by the heartbeat to the naked eye. To achieve this, this work used spatial and temporal filtering to reduce noise and extract the desired frequency band. Then, they amplified the filtered signal by a given factor, α , and added it back to the original signal.

After signal amplification, they extracted the heart rate using two different approaches. In the first approach, they extracted the heart rate by calculating the Fourier Transform of the amplified signal, and then the frequency with the highest magnitude was found. The second approach states that the blood flow does not only cause the face color to change, but it also causes the head to move due to the head reaction to the blood induced force. This head movement is not perceptible to the naked eye. However, their amplification method reveals this movement and its signal. Then, the average heart rate is derived from the head motion signal. The second approach was found to be more accurate than the first approach for extracting heart rates. Its accuracy was valid for a variety of skin tones and independent of gender.

2.2 Heart Rate Estimation Using Smart Phone Camera

Smart phones have become a common device and their capabilities and the included technology is dramatically improving. Based on a recent study, a smart phone can be used as an easy, accurate, and reasonable health monitoring device for vital signs. In addition, it is not confined to the medical environment. Novel methods have been introduced to measure the vital signs using a smartphone in contact with a person and from a distance [6].

Three different techniques have been used to extract the heart rate using either a smartphone's accelerometer, video recording of a finger, or a face. These techniques can be used to monitor the heart rate with the smart phone in direct contact with the person or at a distance. The accelerometer and finger video is considered a method of direct contact while the face video is considered as a distance method [6].

Smart phones have several sensors, such as a 3-axis accelerometer, which can detect any slight motions including the heartbeat. Kwon et al [30] introduced a method to measure the heart rate using an Iphone's accelerometer. They secured the Iphone to the person's chest while the person stands with no major movement. When comparing the results to an Electrocardiogram (ECG), it was found that their method produced comparable results.

The smart phone's camera technology enables the Photoplethysmography (PPG) technique to measure the heart rate variability [6]. This technique is commonly used to measure the heart rate. It is based on data that can be extracted about the changes in blood volume and oxygen from the skin's light reflection. Therefore, PPG can be used to measure the heart rate, heart rate variability, and respiratory rate. For each heartbeat, the blood volume and oxygen increases, which as a result affects the light reflectance. These variations are not distinguishable to the naked eyes. However, a

camera can capture these variations, and then different signal processing algorithms can extract them so that they can be further analyzed. The PPG can be extracted from this light variation.

Several papers present research on monitoring the heart rate using video recordings of the finger tip. For instance, [3], [22], [29], and [34] have introduced novel methods using the PPG technique. To record the video, the examinee puts his or her finger on the smart phone camera such that it covers both the camera and the flash light, which is a Light Emitting Diode (LED) [6]. The LED illuminates to the skin and the camera records the skin color changes caused by blood volume and flow variations.

Scully et al [29] proposed that the smart phone can be used as a precise monitoring device for the heart rate, heart rate variability, respiratory rate, blood oxygen, and heart beat pulse to pulse intervals, which are similar concept to RR intervals (the time between heart beats measured by an ECG device). However, they state that the low sampling rate might restrict accuracy. Lamonaca et al [31] states that current commercial vital sign measurement phone applications should only be used as a reference and not for medical applications.

The face as a source of measuring the vital signs was proposed by Pavlidis et al [32] for the first time in which a thermal camera was used to record a video of the face. Then, Takano and Ohta [33] presented the idea of using an optical camera. This method is more cost effective and easier than using a thermal camera. They extract the vital signs from the face by employing the autoregressive (AR) spectral analysis method to a time-lapsed image, and then measuring the intensity variation on the cheek.

Skin has color fluctuations due to blood flow. When using a smartphone camera, the heart rate extraction is based on these changes in the color intensity of the skin due to blood being pumped to the face or finger with each heartbeat. The intensity or raw

signals, extracted from recorded video, are the result of the mean over either a whole colored frame of the face or of a particular region of the face. As a result of the increase in the size of the region used for color analysis, the signal noise was decreased. However, this process for extracting the heart rate is prone to be inefficient if there is a lot of movement during data recording; therefore minimal movement is needed for success [6].

2.3 Heart Rate Estimation Using Video Camera

Poh et al [25] explained different methods to remotely extract pulse signal by using a video of the face and blind source separation. They discussed that the PPG signal's noise is impacted by the amount of movement which indicates that the PPG signal is very sensitive [25]. This presents a major challenge because the motion noise and the heart rate frequency ranges are very close to each other. Therefore, a linear filter with a cutoff for fixed frequencies would not yield a better result. As a result, they used Blind Source Separation (BSS) more specifically Independent Component Analysis (ICA) for noise reduction. ICA is an efficient noise reduction technique for biomedical signals, including the PPG signal. Further details regarding using ICA as noise reduction technique are discussed by James and Hesse [35].

They used sunlight as the source of light and a laptop webcam to record a video of the face for their experiment. Then, they found the pulse signal and the heart rate using ICA and the frequency analysis methods. Similarly, Kwon et al [3] recorded a face video with 30 frames per second at a 640X480 pixel resolution. They separated the frames into Red, Green, and Blue (RGB) images, and then after normalizing each color ICA was applied to them. As a result, three independent source signals were extracted. Then, the Fast Fourier Transform (FFT) was applied to the PPG signal, which allowed the power frequency in the signal to be found. Once the power frequency was found, the

average heart rate was calculated based on it. When average heart rate was compared to an ECG reading, it was found that there was a good degree of accuracy and precision for the technique performed in the study.

Based on the research in [3], [7], [8], [29], and [34] the raw green signal or the second ICA component resulted in the strongest PPG signal. However, the results of Kwon et al's [3], unlike Jonathan et al [34] result showed that the second ICA component had almost the same or a somewhat worse accuracy than the raw green channel. All the RGB format channels contain a PPG signal. However, similar to the other researchers, Verkruysse et al [8] also showed that the green channel has the strongest signal because hemoglobin absorbs the green light better than red light, and green light penetrates deeper into the skin than blue light.

Lewandowska et al [12] also used day light with the blind source separation method to extract the independent components of the color frame. However, they used PCA (Principal Component Analysis) instead of ICA because it reduced the computational complexity. Once the face is detected, a Region of Interest (ROI) on the forehead is calculated. As shown in Figure 2-1, the ROI is determined based off the distance between the pupils. The ROI is a rectangular shaped with its dimensions and position derived as a fraction of the pupil distance.

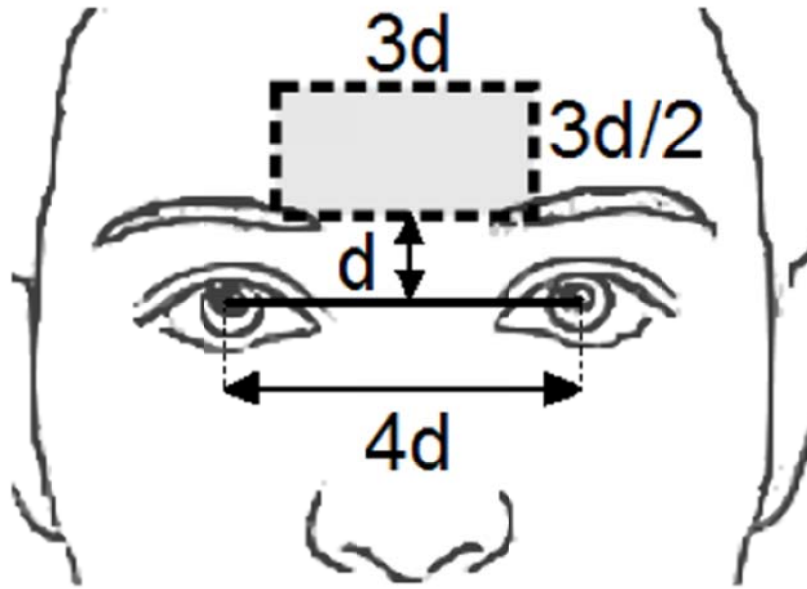


Figure 2-1 The selected ROI [12]

Then, they apply their method on different channel groups: RGB, RG, GB, and RB. They extracted the signal by averaging the ROI pixel of each frame, and then they applied a FIR band pass filter (0.5–3.7 Hz). They used both FastICA – an ICA based function, and the MATLAB `processpca` function – a PCA based function to analyze the signal. As a result, they concluded that both methods have similar accuracies. However, the PCA had better performance in terms of processing speed. They also found that the RG channel group had more accurate results than the other two channel groups. They calculated the heart rate with two different methods. The first method involved extracting the maximum power spectral density function, while the second method involved finding the interval of two consecutive positive sloped zero crossing of the 2nd and 3rd PC [12].

Li et al [18] also extracted the pulse signal from a given number of frames by averaging the green channel values of the ROI for each frame. They showed that the previous experiments techniques could not be applied to the public database, which

includes natural noises such as head movement or changes in lighting. Hence, they introduced a framework that enabled better accuracy by taking into consideration all natural noises sources. They validated this observation by testing their framework using the MAHNOB-HCI public database, a database that includes all natural noises. This framework has three main steps to decrease a variety of noise types. In the first step, they applied the Discriminative Response Map Fitting (DRMF) method to the first frame in order to identify the face model as a ROI, and then the Kanade-Lucas-Tomasi (KLT) algorithm is used to track the region in the subsequent frames. By doing this, they were able to address the problem of head movement. For the second step, they applied the Distance Regularized Level Set Evolution (DRLSE) method to subdivide the background and find a model of light changes by using their average values as a source. Then, they calculated the model's optimization coefficient by applying the Normalized Least Mean Squares (NLMS) filter. By doing so, the impact of the noise caused by light was decreased. For the third step, they segmented the pulse signal and ignored the parts that had high standard deviation in order to reduce the noise caused by head movement.

They used three temporal filtering methods together. One filter is a detrending filter that decreases slow linear or intricate movements into a pulse signal, which can bias the signal time and frequency analysis. Another filter is a moving averages filter. This filter eliminates noises by temporal averaging the sequential frames. A third filter is the Hamming window band pass filter with a cutoff frequency range of 0.7 to 4 HZ. Once these three filters are applied, the Welch's method converts the filtered signal into a frequency, and then the power spectrum density distribution is calculated.

Gregoski et al [36] used a similar method for pulse oximeters for extracting the heart rate, in which oxygenated and deoxygenated blood is measured by infrared light.

Then they extracted the color intensity changes that occurred during a period of time and applied filtering to decrease the noise.

Chapter 3

Background

This section discusses the concepts, algorithms, and methods involved in extracting the cardiovascular parameters from an optical video that have been used in Chapter 4.

3.1 Photoplethysmography

Photoplethysmography (PPG) is an optical technique used to measure the blood volume changes in the blood vessel [4]. Since blood absorbs more light than other biological components in the body, it has been used for noninvasive measurements for cardiovascular system parameters from the skin surface [4]. Examples of such parameters include heartbeat, blood oxygen, and blood pressure [4]. Figure 3-1 illustrates the escalation in blood volume of a blood vessel.



Figure 3-1 The ECG Signal and Equivalent PPG Pulse Signal [4]

There are a number of factors for determining the proper wavelength range for the PPG light source. Visible light spectrum is about between 400 – 700 nm and infrared spectrum is about 700 nm – 1 mm. Water is a major component of tissue and it mostly absorbs the long infrared wavelengths of light. Melanin absorbs short wavelengths of

visible light, such as blue light. However, there is a light spectrum range in the red and near infrared band that passes reasonably well through water. Therefore, these wavelengths are used as a PPG light source for measuring the blood flow. Figure 3-2 illustrates the main tissue absorption spectrum.

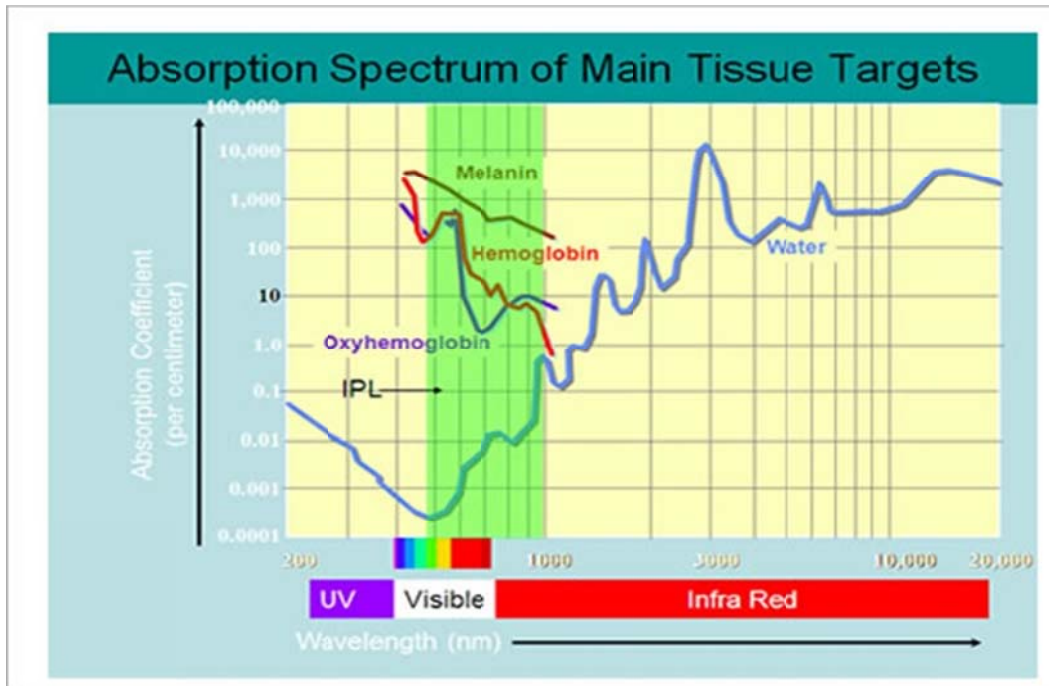


Figure 3-2 Main tissue absorption spectrum. [39]

There is a major difference in light absorption between oxygenated and deoxygenated blood. However, the amount of light absorbed for the infrared wavelength of near 805 nm for these two types of blood is the same, and this point is referred to as the isobestic point. Due to this difference in behavior at different wavelength, the reflected light signal not only contains pulse rate information but also information about blood oxygen changes. Allen [4] elaborates further and includes references about the PPG signal and proper light wave length.

The pulsing behavior of blood is the primary reason for using the PPG technique for monitoring vital signs such as the heart rate and blood oxygen. Furthermore, the amount of light blood absorbs depends on the amount of oxygen in the hemoglobin [17]. Hemoglobin is a protein in blood that transports oxygen from the lungs to other organs. As shown in Figure 3-3, the Oxyhemoglobin and Deoxyhemoglobin absorb light starting from the red range through the infrared range, at wavelengths between 660 nm and 940 nm [11].

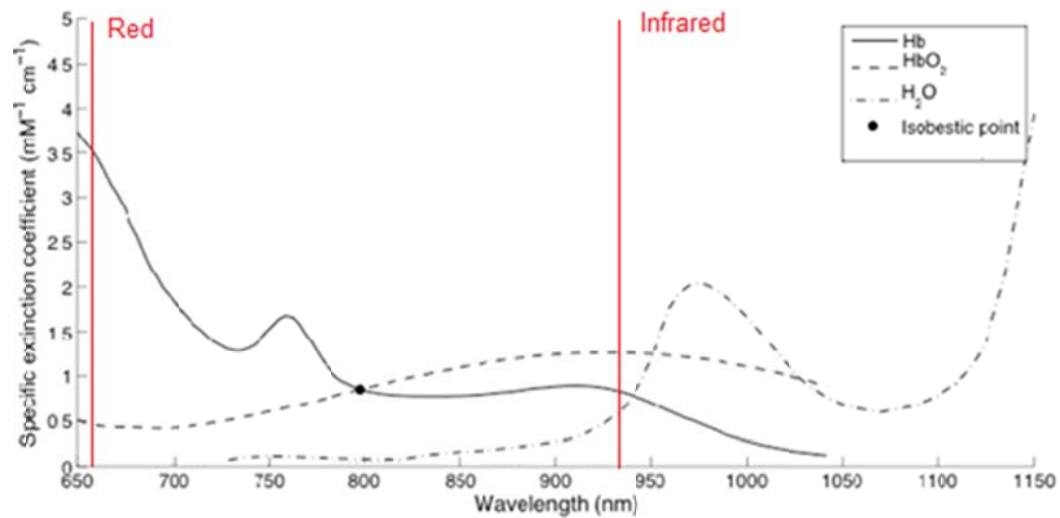


Figure 3-3 Proper red and infrared light wavelength to read PPG signal [27]

The PPG technique has been used for biomedical purposes such as pulse oximeter devices. This device is placed on the person's finger or other part with significant blood flow to measure the heart rate and blood oxygen. A pulse oximeter uses red and infrared wavelengths as a source of illumination and a photo detector sensor to measure the light changes. This device amplifies the changes in light, which are caused by the blood volume changes, by using the light intensity received by the photo detector. Then, after filtering this signal and being converted it into a voltage signal, it calculates the blood oxygen based off the red light to infrared light absorption ratio. Further details

about how a pulse oximeter works and its method to calculate the heart rate and blood oxygen can be found in [17, 28].

3.2 Pulse Wave and PPG signal

For blood circulation to occur, the heart pumps blood through a series of arteries throughout the body. The arteries have a valve like behavior in which upon opening they experience a tensile stress, and then the valve goes back to equilibrium to where it is in its original state. This process causes a local movement of blood at the arteries, which ultimately causes a pressure change. The change in pressure causes the blood to flow from one artery to another artery, where another local movement of blood occurs because of the valve like behavior. Essentially, the local movements of blood causes pressure changes which causes the blood to flow throughout the body. These pressure changes are the driving force for blood flow. Furthermore, when a pulse wave passes through the arteries, three parameters can be detected: blood flow or flow pulse, a rise in blood pressure or pressure pulse, and the volume pulse.

The most common way to measure the blood volume and blood pressure is the PPG technique. Diagnostics based on the PPG signal have three steps: preprocessing the PPG signal by removing the noise, extracting the PPG signals features, and signal classification and diagnosis. Important information, such as the cardiac performance, the arteries' elasticity, pulse stability, and sudden changes in the waveform, can be extracted by analyzing the profile shape of the volume pulse signal. One way of extracting the features and parameters from the PPG signal is to analyze the profile of the blood volume signal. Figure 3-4, shows the general shape of the volume and pressure pulse wave.

This wave consists of two parts: systolic and diastolic. The features of this pulse include: the amplitude of the systolic and diastolic peaks (AP1 and AP2), total duration of the

pulse wave (TPT), the time from the wave's start point to the first peak (TP1), time of the wave's start point to the second peak (TP2), and finally the inter-wave time of the systolic peak (IWT).

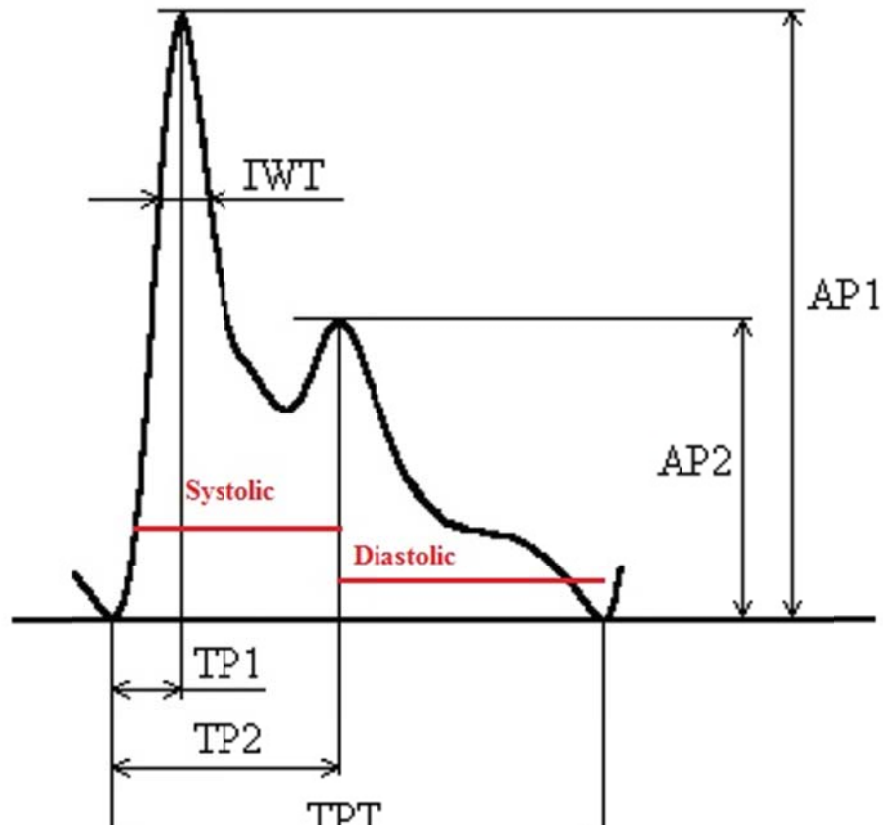


Figure 3-4. Volume and pressure shape and features [14]

3.3 Infrared wavelength

Studies have been performed for finding the proper red and infrared wavelength needed to extract the PPG signal. It was found that 660 nm was the proper wavelength for red light, while the 880, 910, and 940 nm wavelengths were the proper wavelengths for infrared light [5].

In the body, water as well as oxygenated and deoxygenated hemoglobin absorbs the majority of the infrared and visible light wavelengths. As shown in Figure 3-5, the infrared wavelengths within the range of 650 and 950 nm are absorbed by hemoglobin. Water mostly absorbs the infrared light wavelengths higher than 950 nm. Therefore, the light wavelengths between the range of 650 nm and 950 nm can be used for measuring the heartbeat parameters.

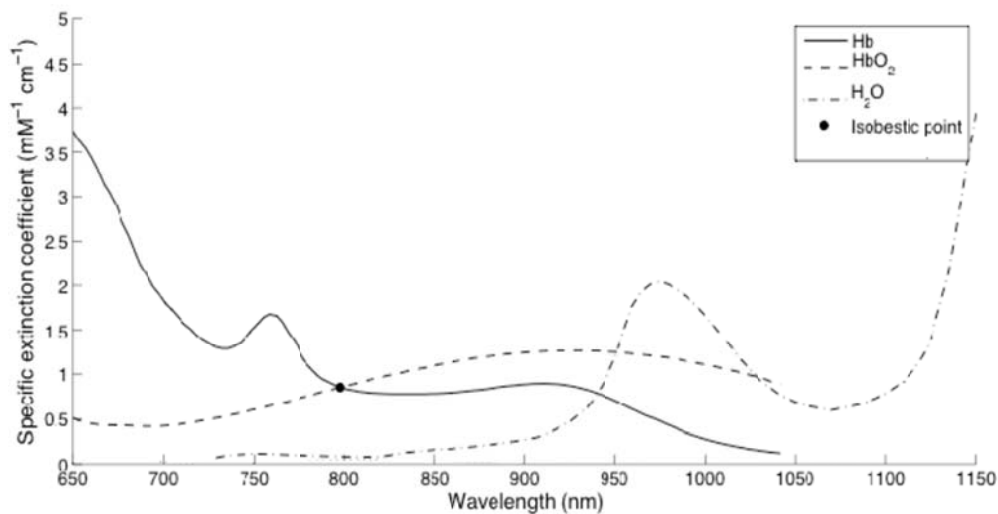


Figure 3-5 Water (H₂O), Oxygenated hemoglobin (HbO₂), and Deoxygenated hemoglobin (Hb) light absorption spectrum in the near-infrared range [27]

In Figure 3-5, the isobestic point, the point where the wavelength of the Hb and HbO₂ light absorption spectra are almost equal, occurs at approximately at the 800 nm wavelength [27]. At this point, the reflected light is less affected by blood volume changes.

3.4 Signal Processing

The following sections explains the signal processing algorithms that have been used in this study to extract the PPG signal from the face frames, process the extracted signal to reduce noise, and finally calculate the heart rate.

3.4.1 Face Recognition

The three techniques of face recognition, facial feature extractions, and tracking were used on video recordings to locate the face, find facial features, and to track stable regions in order to produce a PPG signal. For this experiment, the face was recognized using the vision.CascadeObjectDetector System object from Matlab version R2014b's Object Detection and Recognition Toolbox [37]. This system used the Viola-Jones algorithm for object detection. This algorithm allowed detection of the face by default, but it also allowed detection of other objects such as the eye, nose, mouth, and a person's upper body.

The Viola-Jones algorithm [38] is a fast machine learning algorithm which processes images and detects most visual objects. This algorithm has three important factors. The first factor is Integral Image, an image analysis method which improves the computing of features used for detection. The second factor is a learning algorithm based on the AdaBoost algorithm that achieves remarkably effective classifiers. This allows a trivial number of important features to be chosen from a broader group of visual features. The third factor is a technique used to gradually chain more complicated classifiers in a cascade. This technique allows the unwanted background area of the image to be rapidly discarded, and it focuses more on the area that is more likely to be the object. Cascade differs from the previously used approaches in the sense that it concentrates on the object area of interest instead of using statistical assurance to reject the area which is less likely to include the object.

The process of the Viola-Jones algorithm is similar to the basic Haar technique which utilizes a set of features. It uses integral image to quickly evaluate features at several scales. The features can be calculated in constant time at any area or scale. Since the total number of features is numerous in any image, a learning algorithm

discards a majority of them and concentrates on a minor number of relevant features in order to guarantee a quick classification. This algorithm uses a variation of AdaBoost, a cascade technique, both for choosing a few features and then for training the classifier. For a given image during the first few steps of object recognition, the cascade keeps the positive area as small as possible, while it eliminates the negative area as much as possible.

3.4.2 Face Feature Extraction

I used Discriminative Response Map Fitting (DRMF) [20], a method for Constrained Local Models (CLM), to extract the features from the face and find the region of interest. This method is known for good performance in fitting a model to different general faces [18].

In this method a small group of parameters can indicate the response map. An unknown response map can be realistically recreated based on the extracted probability response map dictionary. In addition, the method uses an accurate function that can extract a response map based on the shape parameter updates by applying regression methods.

DRMF is a facial transform model that extracts the facial shape which is detected by a set of parameters from an image. These types of models can be classified into two major groups. The first group includes Holistic Models which are based off of texture-based facial features. The second group includes Part Based Models which are based off of local image areas. The CLM is a part based Model, and is represented by model $M = \{S, D\}$ with S being the shape models and D being different facial feature detectors. Each part of D corresponds to a point from the shape model. The part based model has two major advantages. One advantage is that some of the obstacles can be simplified since only part of the facial features is under consideration. The second advantage is the ability

for connecting simplified 3D facial shapes because no complex image function needs to be calculated.

Regularized Landmark Mean-Shift (RLMS) is another method for the CLM model [18]. This method looks for the maximum probability of a recreated shape based on the assumption that all facial features are located in the image. RLMS differs from DRMF in the sense that DRMF uses a biased regression to approximate the model parameters [18].

In the DRMF training process, an initial step is to acquire a dictionary of a response map probability in order to find important features for updating the fitting model. The next step involves extracting the updated fitting model through iterations by using an adapted boosting method. The boosting method involves sampling the 3D model parameter near a known boundary that is closed to the exact parameter. Then through iterations, it models the correlation between the shape that was sampled and the parameter update.

3.4.3 KLT Point Tracking algorithm

The Kanade Lucas Tomasi (KLT) algorithm [21] is a tracking point algorithm in which a window of pixels with adequate texture is used for tracking instead of a single pixel. The term adequate texture refers to the fact that not all image patches have motion data. As a result, it is desired to use windows that include motion data; these windows include corners, pixels with high spatial frequency values, and a combination of adequately high second order deviations.

One of the advantages of KLT algorithm is its guarantee to track the same window if its component has moved over time. It does so by checking the window appearance regularly to see if a window appearance has significantly changed, and it will be excluded if it has changed. The second advantage of the KLT algorithms is that it uses

a compound transposition instead of a simple one. As a result, different points of a window can be related to different movements.

3.4.4 Temporal filtering

In order to decrease the pulse's signal noise, temporal filtering is employed and it eliminates the frequencies that are outside of the heart rate range. The natural range of the heart rate is 0.7 to 4 HZ, which is equivalent of 42 to 240 bpm.

Many temporal filtering methods have been introduced to decrease the noise of the pulse signals for heart rate measurements in related papers such as [18], [19]. In this study I used a Butterworth filter, which is an Infinite Impulse Response (IIR) filter.

3.5 Heart Rate Variability

The heart rate is one of the most important cardiovascular parameters to extract from the PPG signal. The heart rate refers to the number of heart beats per minute (bpm). Bpm is also used as the unit of measure for heart rate. This parameter is important because it needs to be monitored for cardiovascular diseases. Physical exercises and mental stress can have a high impact on the heart rate. As a result, it is important to monitor the heart rate regularly [6].

Heart rate variability (HRV) is another important cardiovascular parameter that can be measured from the PPG signal. HRV refers to the changes between heart beats with respect to time. The frequency range of HRV can vary. The HRV frequency of a healthy and young person usually is at the respiratory frequency (RSA), which occurs approximately between 0.15 Hz to 0.4 Hz [16]. However, for infants or an adult that is exercising, this range can be below 0.15 Hz or above 1 Hz [16].

The pulse to pulse interval, the time between two consecutive heartbeats, is one of the features of the PPG signal that can be used to measure the heart rate. This feature fluctuates at a low frequency approximately between 0.05 to 0.15 HZ [16]. The sample of

HRV is measured at the peak of the PPG signal. The value of each sample is calculated by the inverse of the pulse to pulse interval.

The frequency range of HRV is usually classified in three groups. The first group is Very Low Frequency (VLF), which includes frequencies between [3.3, 40] mHz. The second group is Low Frequency (LF), which includes frequencies between [40, 150] mHz. The third group is the High Frequencies (HF), which includes frequencies between [150, 400] mHz. Pulsation in any of these frequency ranges has biological implications.

Chapter 4

Technical

The purpose of this work is to extract the heart rate, heart rate variability, and blood flow signals from a raw PPG signal. In the following section, I explain the method developed, the environment of the experiment, and the process of extracting the ROI and PPG signal in detail, and finally present and discuss the comparison of the results using visible and infrared illumination for two subjects.

Each person has a unique range of normal heart rates. The heart rate will increase after exercise or normal activity. Therefore, the normal heart rate should be taken into account when monitoring and interpreting a person's heart rate. There are important factors that affect the output of visual heart rate analysis algorithms and as a result it is important to take them into account. These factors include: the amount of light, the subject's head movement, and the subject's physical parameters such as, age, and skin tone. To address these factors in the experiment, the following was done: the amount of light was controlled and the head movement was minimized as much as possible. The two subjects were young, one subject wore glasses, and the two subjects had different skin tones with one being light and the other being dark.

It is important to note that there are some factors or scenarios that cause this technique of monitoring the heart rate to produce inaccurate results or no result at all. If the subject's head moves too much, the error check in tracking the ROI would fail to solve this problem. To address this, I repeated the process of finding the face, facial features, and ROI; however when there was a lot of head movement, this additional analysis slows down the overall process significantly. The second factor that can produce inaccurate results or none at all is lighting. If the amount of light is not controlled to the

point where there is adequate light, the camera will be unable to detect changes in light reflection from the face.

As a result, there are certain requirements needed in order to get an accurate result for this experiment. These requirements include: the subject looking straight into the camera, that there is no major movement causing the face to move out of the face box, and that the subject remains looking relatively straight in the direction of the camera so that the ROI is not lost.

4.1 Environment

The experiment to evaluate the method introduced here was conducted using two different environments. The first environment used infrared illumination by using four infrared LEDs as a source of light. These LEDs were placed at four corners of a frame and they were pointing towards the face. The video was then recorded with this environment using a camera and a filter which only passes 940 nm-- a wavelength that is mostly absorbed by oxygenated blood. A second environment used lighting from the visible spectrum. For this environment, the camera used an infrared filter to record RGB video, which prohibited the infrared wavelengths to pass through.

In both cases, the video was captured indoors. A 40 second video was captured using a GoPro Hero4 Camera in 1280X960 resolution and 120 frames per second. The captured video was then saved in the high quality AVI format, which is a compression-less format [12].

4.2 Region of Interest Detection and Tracking

Three regions of the face were chosen for extracting the PPG signal: the forehead and both the left and right cheeks. First, I applied face recognition to find the face on the first frame using the Matlab Viola-Jones algorithm, which is commonly used to detect faces. Then, I used the Li et al implemented framework [18] and applied the

DRMF method [20] to extract facial features in a set of points on the face frame. The DRMF output consists of an array with a total of 66 points. The points are distributed to specific facial features or components, and the distribution includes: the first 17 points for the face, then the next 10 points are for the eyebrows, the next 9 points are for the nose, the next 12 points for the eyes, and the remaining 18 points are for the mouth. Figure 4-1 shows the extracted features.

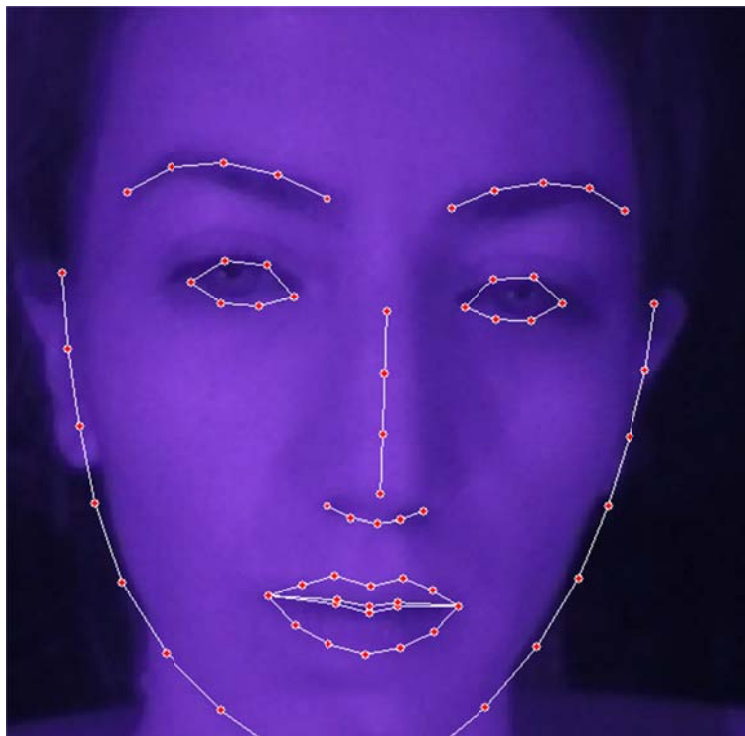


Figure 4-1 Face recognition, feature extraction

In order to define the ROI, two features with the most stability were chosen from the face. The nose and eyebrows were chosen out of all the extracted facial features because the other points on the face were significantly lost due to the head movement, the eyes' points were significantly lost due to blinking, and finally the mouth's points can potentially get lost due to mouth movement. Four points on these two features were then

used to determine the ROI. Each ROI was denoted by a width of 40 pixels and a height of 80 pixels. Figure 4-2 shows the selected features and the calculated ROI.

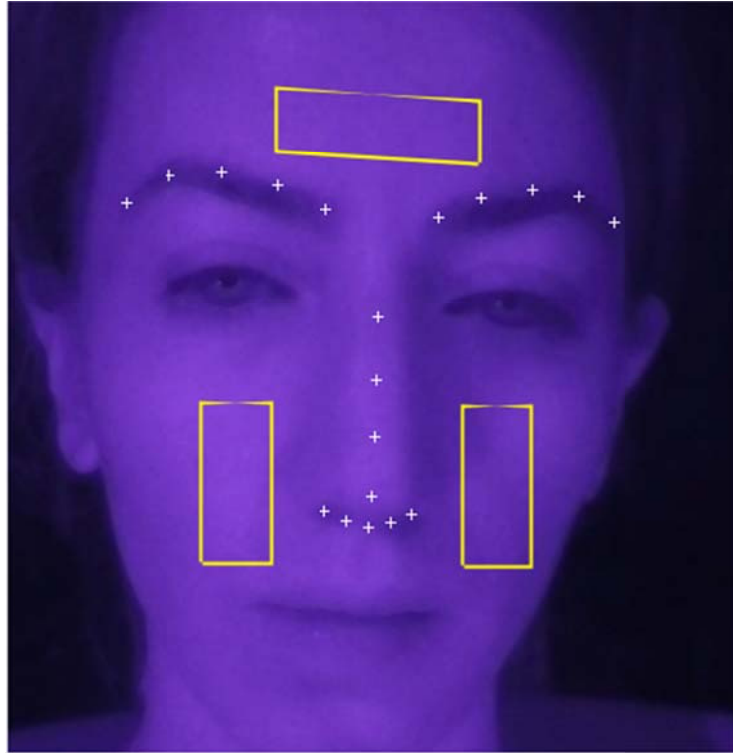


Figure 4-2 Selected Features and ROI

Next, I used the Matlab KLT algorithm to track the particular facial feature points in the following frames. I define two groups of points for tracking: one for nose's points and another for the eyebrows. I chose these two groups of points because these two parts had the least movement and the lowest rate of occlusion and failure to track and thus they were the most stable. I only detected the points using DRMF once during the first frames, and then tracked them during the rest of the frames. However, I checked the error by counting the lost points during the tracking and to see whether the error was high. If a high error occurred, I extracted the features again for that frame, and then reset the point tracker with the new points. Then I extracted the registered ROI. By doing so, I

was able to track the ROI and address the issue of head movement to a certain degree [18]. I averaged the intensity values of each region in each frame, and then concatenated them in the time sequence in order to extract three raw PPG signals.

4.3 PPG Signal Filtering

The quality of the output can be diminished by video frame noise, head movement, and light noise. The video frame noise is caused by the camera sensor. Considering that the value of one pixel generates a very noisy signal, a small window of pixels is required for the ROI in order to keep noise at a minimum. The average of the pixels' values for that window through the sequence of frames creates a signal.

The raw PPG signal extracted from both the RGB and infrared video still had a degree of various noise due to movement and illumination. In order to extract the heart rate, different frequency ranges other than the frequency range of the heart rate needed to be filtered. Therefore, I applied Matlab's second order Butterworth filter to extract the [0.7 4] heart frequency range of interest. Butterworth compare to other linear filter has maximally flat magnitude, and it has no ripple. It also rolls off more slowly. I set the cutoff frequency to $[0.7/\text{fps} \times 2, 4/\text{fps} \times 2]$, with fps referring to the frequency of the recorded video.

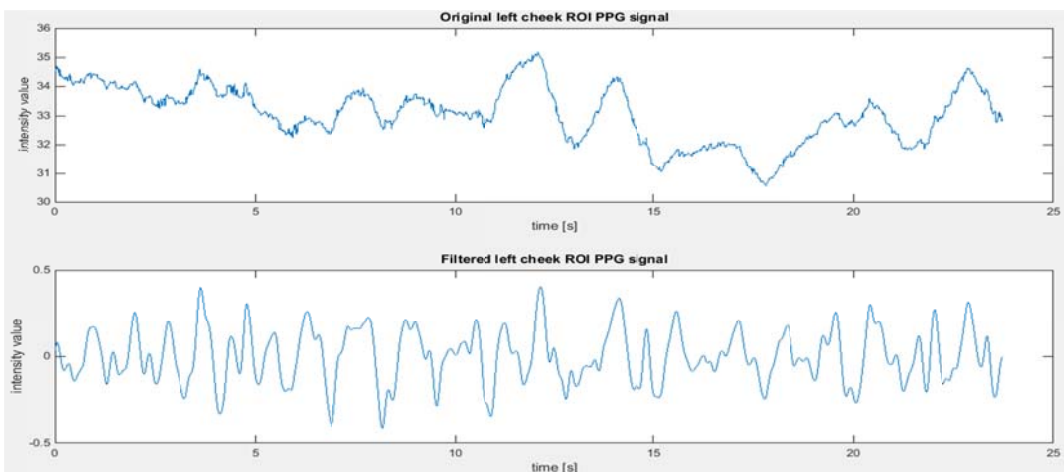


Figure 4-3 Left Cheek ROI original and filtered signal

A sample of the raw PPG signal from the three ROIs and the output after applying the Butterworth band pass filter on them are shown in Figures 4-3, 4-4, and 4-5.

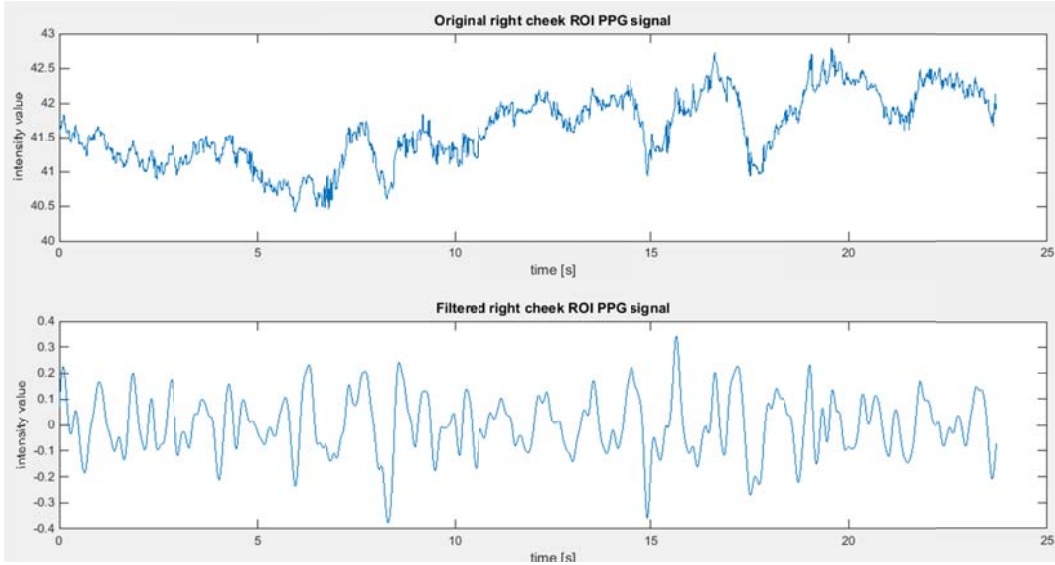


Figure 4-4 Right ROI original and filtered signal

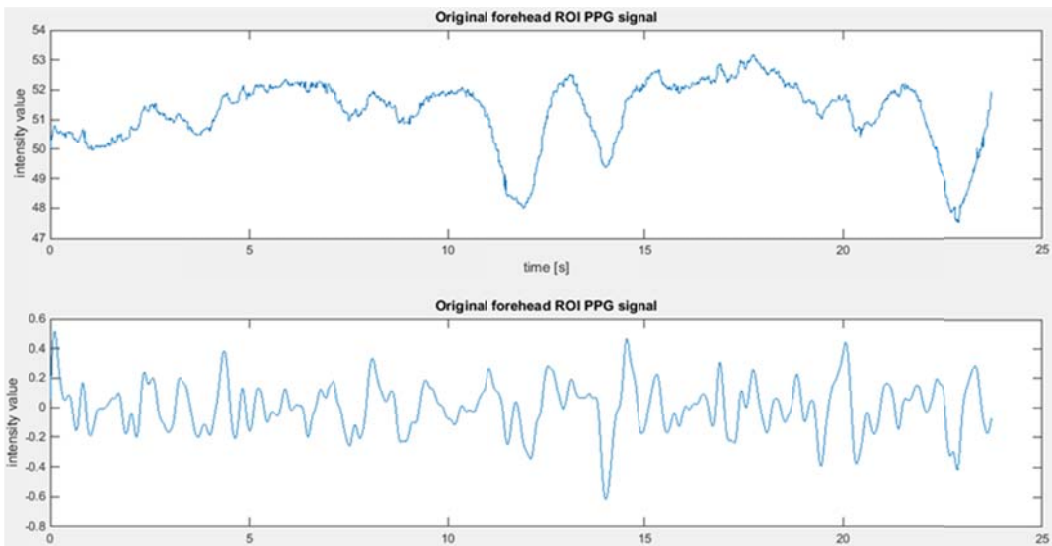


Figure 4-5 Forehead Cheek ROI original and filtered signal

4.4 Heart rate

In order to calculate the heart rate, I applied Mellado [22] sliding window frequency analysis. Every half second and full second, I continually estimated the heart rate on a PPG signal window for a recorded video of 120 fps. By doing so every half second, the time resolution of the output was improved without any effect on the output accuracy. For a recorded video with 120 fps, the PPG signal window length for heart rate calculation is 12 seconds. The length of window is important because it impacts the quality of estimation. The 12 second window is equivalent to a 5 bpm frequency resolution. The frequency resolution, F_r , of a signal is the frequency between two sequential samples. The signal FFT is sampled N times with a sampling frequency F_s . Therefore, the frequency between two sequential samples is F_s/N , which results in the window time length. In Equation (1), the F_r is the frequency resolution, F_s is the sampling rate, N is the number of window samples, and T is the duration of a time window.

$$F_r = F_s/N = N/T/N = 1/T \quad (1)$$

Normally when a continuous signal is cut into discrete samples and then a continuous function is created, the accuracy of the results becomes dependent on the sample rate of the original signal [24]. In this experiment, the heartbeat corresponds to the signal being cut into discrete samples, and the discrete sample corresponds to the magnitude of the signal in each frame. The Nyquist–Shannon sampling theorem specifies to use a particular sampling rate so that accuracy is maintained and no information regarding the continuous signal is lost [24].

Based on the theorem definition, if a time signal $S(t)$ does not have any frequencies higher than F Hertz, it can be accurately represented by a series of samples $1/2W$ apart [24]. Therefore, the adequate sample rate is $2F$ or greater. The Nyquist–

Shannon sampling theorem applies to signals with limited frequency ranges [24]. This means that the Fourier Transform of these signals is zero outside of their frequency range [24]. Discrete Fourier Transform (DFT) is a mathematical technique to convert a function from the time domain to the frequency domain.

The PPG signal is filtered using a band pass filter in order to eliminate frequencies that are not of any interest, such as any frequency outside the heart rate range of between 0.7 to 4 Hz., Therefore, the filtered PPG signal from a ROI fulfills the Nyquist-Shannon sampling theorem's required criteria, and as a result, it can be applied to this signal, which requires the adequate sampling rate to be at least twice the upper frequency limit. In this experiment, 4 Hz is considered to be the upper limit of the frequency for the heart rate frequency range, and therefore the sampling rate should be at least 8 Hz in order to record the whole range of heartbeat frequencies without aliasing. In this experiment with the GoPro black Hero4 camera, the videos are recorded at 120 frames per second, which is about 15 times of the desired frequency.

The next step is the heart rate estimation for each signal window. First, I converted the time domain signal window to the frequency domain using the Discrete Fourier Transform (DFT), by using Matlab's FFT algorithm. The second step involved detecting the peak.

DFT is designed to be applied to an infinite time signal. Therefore, the result of DFT is a time signal with N components, and the signal continues because of infinite time, which causes spectral leakage. Leakage typically is the result of windowing. When sampling and windowing are both applied to the time signal: the leakage caused by windowing contributes to a localized spreading of the frequency components which often causes a blurring effect, while aliasing is a periodic repetition of the entire blurred spectrum caused by sampling.

To decrease spectral leakage, a side effect of windowing, the DFT time signal input is multiplied by a window function with boundary values of zero [22]. The Hann window is one of these types of window functions. This function has a decent leakage refusal and resolution between others.

To detect the peak in the frequency signal, I used a Matlab function. This function found the local maximum, which means it detects the largest peak within a defined domain. The peak with the maximum amplitude is selected and then transformed to beats per minute (bpm). The calculated average heart rate for the windows is the mean heart rate for the person during the captured video. A sample of the frequency analysis of the PPG signals for the average of the three ROI and the output heart rate signal are shown in Figures 4-6.

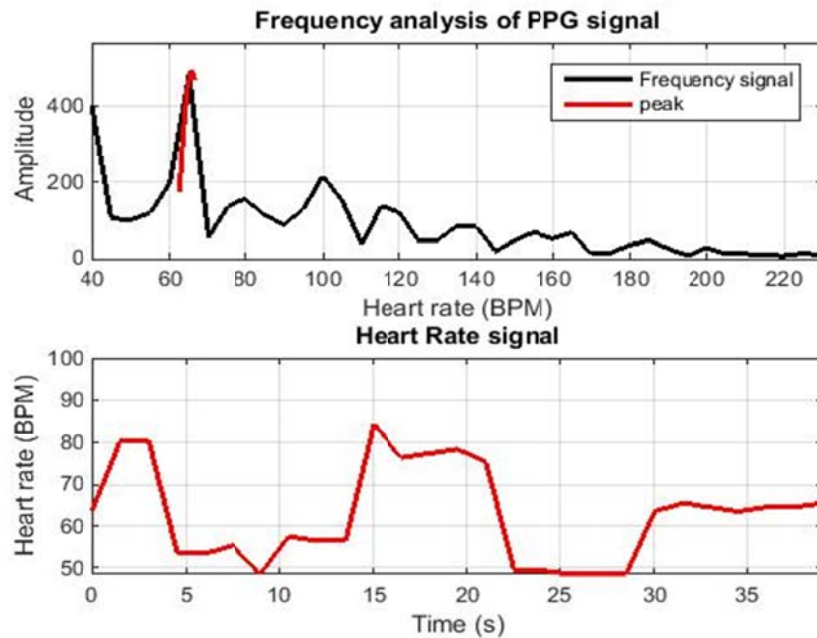


Figure 4-6 Frequency analysis of the PPG signal and the output heart rate signal. The mean heart rate is 65.45 bpm

Next, using the mean heart rate (MHR) that was found, I found a sharper cutoff for the Butterworth filter, $[(MHR-10)/60 \text{ } (MHR+20)/60]$, and I calculated the mean heart rate again. As a result of this adaptive band pass frequency selection process, the accuracy improved significantly for all the outputs. Figures 4-7 shows the output frequency analysis of the filtered PPG signal and the heart rate signal after the adapted band pass filtering.

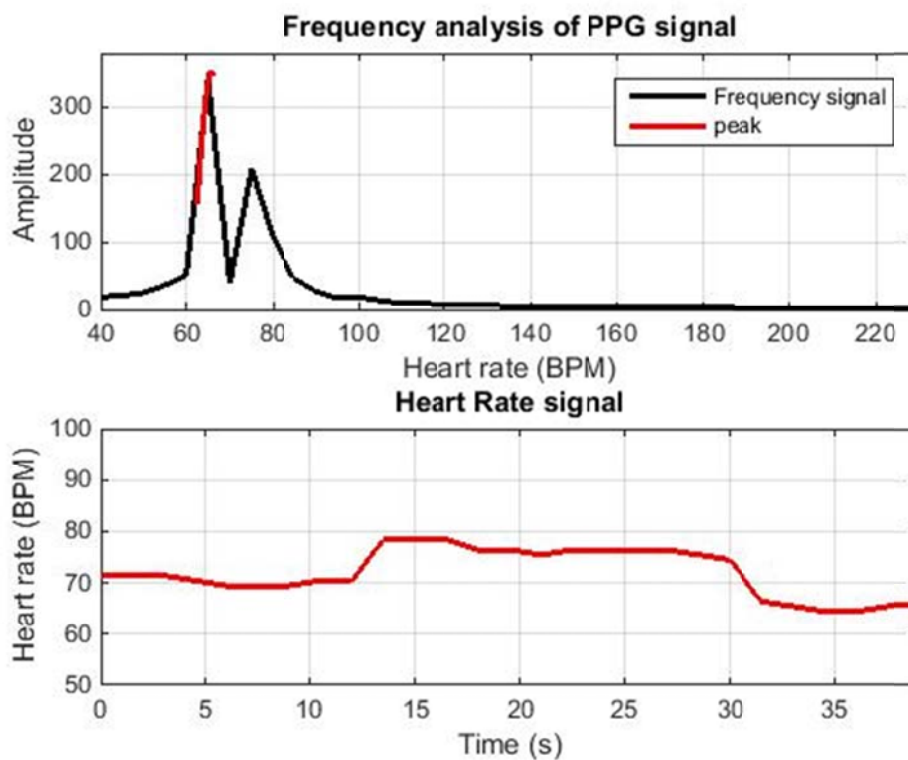


Figure 4-7 Frequency analysis of the PPG signal and the output heart rate signal. The mean heart rate is 78.88 bpm

This method was applied to the videos using both infrared and visible light. I extracted the signal from the green and red channels for the video using visible light and the only channel for the video using infrared light. Table 4-1 shows the result of signal extracted from a 120 fps video from a light skinned subject.

Table 4-1 the result of the signal extracted from a 120 fps video from a light skin subject.

The most accurate mean heart rate and the standard deviation are shown in red.

Red Light		Green Light		Infrared		pulse oximetry
[0.7 4]	[0.94 1.44]	[0.7 4]	[0.91 1.46]	[0.7 4]	[1.04 1.37]	
70	70	70	71	46	79	67
61	71	79	71	46	79	67
70	70	80	70	46	79	70
69	69	69	69	46	79	71
66	81	68	68	46	78	72
66	68	55	68	46	77	72
66	68	66	67	80	76	72
66	68	65	68	46	76	73
64	69	64	70	79	75	74
64	69	56	70	46	74	74
65	69	84	84	45	74	75
60	75	59	84	45	76	75
59	73	59	77	45	71	75
59	72	80	77	64	71	76
58	71	77	77	63	71	76
58	71	49	78	44	70	76
71	71	49	78	95	70	76
71	71	48	77	44	69	75
70	71	58	76	44	69	75
70	70	57	75	45	69	79
70	79	74	75	61	68	79
98	79	56	74	69	70	79
55	75	64	74	94	70	80
55	75	63	75	94	76	80
74	74	64	75	94	76	80
64	74	64	74	95	76	79
64	74	65	74	96	76	79
66.49	71.08	64.97	74.37	72.59	74.3	75.03
12.11	4.52	14.298	4.542	24.41	3.81	

The heart rate in this result was estimated every second for a window of 12 seconds and the total video length was 40 seconds. To represent this, each row lists the results for one 12 second segment and rows from top to bottom represent intervals of 1 second.

The first column for each spectrum is the heart rate estimation from a Butterworth filtered signal with the broader cutoff factor, which is [0.7 4]. The second column is the heart rate

estimation from the Butterworth filtered signal with the sharper cutoff according to the found mean heart rate (MHR) from the first column. The last two rows are the mean heart rate over the estimated heart rates sample and the standard deviation of the estimated heart rates for all used 12 second segments with the actual mean heart rate, respectively.

In this experiment, the most accurately calculated mean heart rate that resembles the actual mean heart rate is the output of green light channel and infrared light. However, infrared light has a lower standard deviation. However, this result has to be interpreted in the context of the very small sample size. The most important aspect that this table demonstrates, however, is that the heart rate results with the second, heart rate adaptive band pass filter is more precise and has significantly lower variance than the one obtained with only the generic filter. This applies to all light wavelength choices and all skin regions used.

Table 4-2 shows the same result of signal extracted from a 120 fps video from a dark skin subject. The heart rate in this result is again estimated every second for a window of 12 second and the video total length was 40 second. In this experiment, the mean heart rate that is the closest result to the actual mean heart rate is the output of green light channel and infrared light. However, infrared light has lower standard deviation. Again, results with the adapted band pass filter are more precise and have lower variance.

Table 4-2 the result of signal extracted from a 120 fps video from a dark skin subject.

The most accurate mean heart rate and the standard deviation are shown in red.

Red Light		Green Light		Infrared		pulse oximetry
[0.7 4]	[1.25 1.75]	[0.7 4]	[1.21 1.71]	[0.7 4]	[1.04 1.54]	
52	83	96	84	65	71	79
83	83	94	84	54	71	79
84	84	94	84	90	75	79
95	84	94	84	68	74	79
94	84	94	84	68	74	75
95	83	94	84	68	74	75
94	82	94	84	58	74	80
93	82	93	83	58	74	80
100	83	92	83	71	74	80
100	83	93	75	71	74	80
99	90	93	74	58	74	80
99	91	93	74	59	74	78
101	84	95	74	60	74	79
90	84	89	74	60	74	80
89	87	75	76	61	73	80
86	86	74	76	61	72	79
86	86	99	76	61	78	79
86	86	67	76	70	78	79
84	85	66	76	70	71	75
85	85	69	75	59	70	75
103	84	68	76	86	70	75
103	84	70	84	85	70	76
60	84	69	84	85	70	76
59	84	69	84	104	71	76
60	84	69	76	103	71	76
59	84	59	75	101	71	79
59	84	59	75	101	71	79
85.55	84.99	82.7	79.48	72.85	73.3	78.03
17.14	6.83	14	4.45	16.53	4.22	

HRV is another parameter that can be extracted from the peak of the sharper filtered signal. The magnitude of each sample is calculated as the inverse of the time difference between consecutive pulse peaks. Figure 4-8 shows an example of sharper filtered signal, the corresponding autocorrelation results of the first 24 second of the filtered signal, the extracted HRV signal from sharper filtered signal, and the distribution for the same HRV signal. The first two figures in Figure 4-8 show the strong periodicity and distinct peaks in the sharper filtered data. The second two figures in Figure 4-8 show the HRV temporal progression as well as the HRV distribution. Considering only the peak of the HRV signal on the left, a histogram can be constructed which shows the pulse to pulse distribution [40].

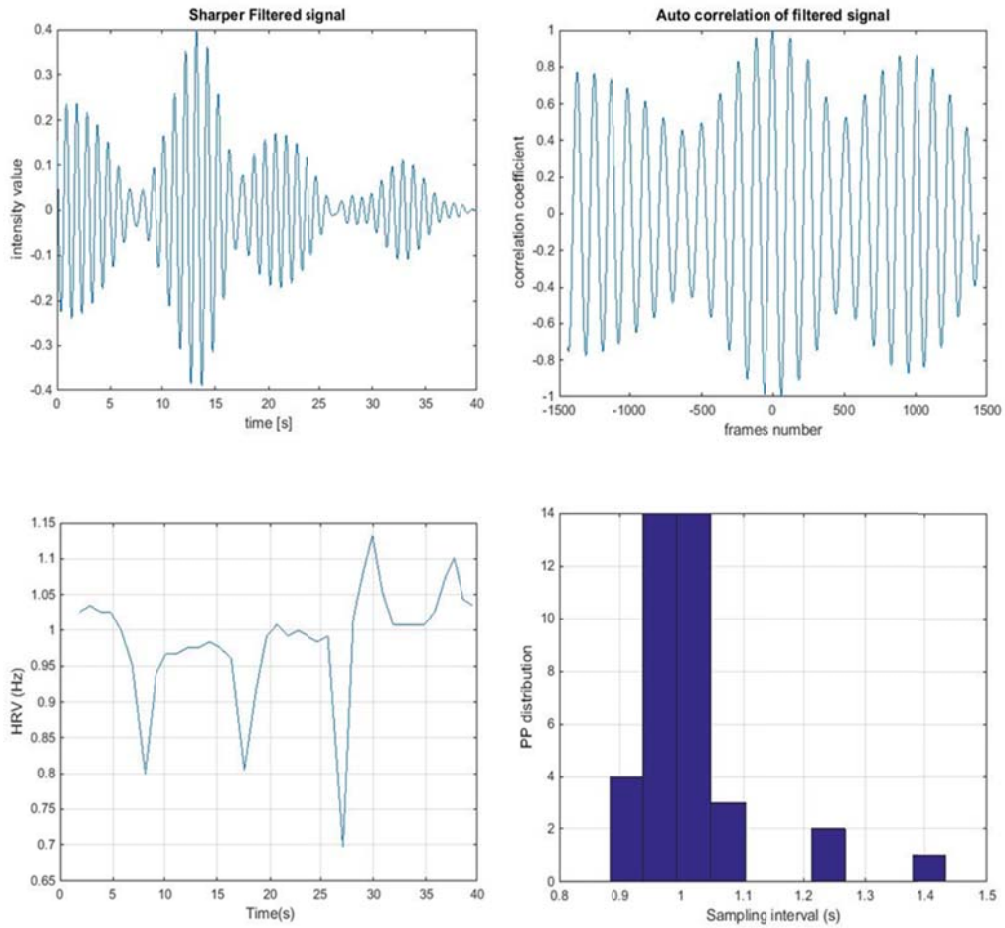


Figure 4-8 an example of sharper filtered signal, the corresponding autocorrelation results, the extracted HRV, and the distribution for the same HRV signal.

Conclusion and Future Work

Being able to monitor vital signs non-intrusively and autonomously is important for early diagnosis as well as disease management. In this thesis, a system for the autonomous tracking of heart rate and blood flow has been presented and results at multiple light wavelengths have been analyzed. The experimental results show that modifying the filter cut off frequency dynamically based on the found mean heart rate from the broader filtered signal has important role in finding the more accurate mean heart rate. It means the deference of heart rate samples from actual heart rate is less and as result the estimated mean heart rate is more accurate compare to actual mean heart rate. It also indicates that the infrared environment with its simpler way to control lighting has lower standard deviation in the dark skin subject as well as in the light skinned subject. In both cases the infrared light result had the lowest standard deviation. However, the closest mean heart rate to the actual mean heart rate is in green light outputs in the light skin and dark skin results. While the sample size was very small, this might indicate the potential of multiple wavelength analysis for better results.

The next step in future work, based on having the signal of three ROIs in the face, is to extract the exact shape of the blood flow signal. In this experiment the signal is filtered using the sharper cutoff to extract the heart rate. However, the details of the shape of the signal are contained in the higher frequency. Therefore, the signal should be filtered with a wider filter to preserve more shape information. This, however, increases noise and a different way to reduce noise has to be found. In addition, the signal is extracted from the average of the whole window. Averaging of the signal over a large region will filter temporal differences of different regions, thus altering and eroding the shape information. Therefore, the ROI window should be divided into smaller regions. By

using smaller regions, more details such as the time shift of the signal can be extracted allowing the approximate shape of the signal and finer grained blood flow to be found.

References

- [1] Wu H., Rubinstein M., Shih E., Guttag J., Durand F., and Freeman W. Eulerian Video Magnification for Revealing Subtle Changes in the World. *ACM Transactions on Graphic (Proc. SIGGRAPH 2012)*, 31(4), 2012. doi:10.1.1.412.9637
- [2] Balakrishnan G., Durand D., and Guttag J. Detecting Pulse from Head Motions in Video. *IEEE*, 2013. doi:10.1109/CVPR.2013.440
- [3] Kwon S., Kim H., and Suk Park K. Validation of Heart Rate Extraction using Video Imaging on a Built in Camera of a Smartphone. *IEEE*, 2012. doi: 10.1109/EMBC.2012.6346392
- [4] Allen J. Photoplethysmography and its Application in Clinical Physiological Measurement. *PHYSIOLOGICAL MEASUREMENT*, 28 (2007) R1–R39. doi:10.1088/0967-3334/28/3/R01
- [5] Nguyen W., Horjus R. Heart-Rate Monitoring Control System Using Photoplethysmography (PPG). *Senior Project ELECTRICAL ENGINEERING DEPARTMENT California Polytechnic State University*, 2011.
- [6] Rafael S., Monitoring Heart Rate with Common Market Smart-phones for Identifying Potential Signs that may Lead to Sudden Death., *Blekinge Institute of Technology*, September 2013.
- [7] Poh M., McDuff D., Picard R. A Medical Mirror for Non-contact Health Monitoring. *ACM SIGGRAPH Emerging Technologies*, 2011.
- [8] Verkruyse W., Svaasand O L., and Nelson J S. Remote Plethysmographic Imaging using Ambient Light. 16(26): 21434-21445, 2008.
- [9] Chambino B P. Android-based Implementation of Eulerian Video Magnification for Vital Signs Monitoring. *FACULDADE DE ENGENHARIA DA UNIVERSIDADE DO PORTO*, 2013.

- [10] Su R., Dockins T., Huber M. ICA Analysis of Face Color for Health Applications. *Association for the advancement of Artificial Intelligence*, 2013.
- [11] Mengelkoch L.J., Martin D. and Lawler J., A Review of the Principles of Pulse Oximetry and Accuracy of Pulse Oximeter Estimates During Exercise. *Physical Therapy*, 74(1):40-49, Jan. 1994.
- [12] Lewandowska M., Rumiński J., and Kocejko T. Measuring Pulse Rate with a Webcam – a Non-contact Method for Evaluating Cardiac Activity. *IEEE*, 2011.
- [13] Hyvarinen A., Survey on Independent Component Analysis. *Neural Computing Surveys*, 2: 94–128, 1999.
- [14] Korpas D., Halek J., Dolezal L. Parameters Describing the Pulse Wave. *Physiol*, 58: 473-479, 2009.
- [15] Nenova B., Iliev I. An Automated Algorithm for Fast Pulse Wave Detection. *INT. J. BIOAUTOMATION*, 14(3):203-216, 2010.
- [16] Berntson G. G., Bigger JT. Jr., Eckberg D. L., Grossman P., Kaufmann P. G., Malik M., Nagaraja H. N., Porges S. W., Saul J. P., Stone P. H., VAN DER Molen M. W. Heart rate variability: Origins, methods, and interpretive caveats. *Psychophysiology*. 34(6):623-48, 1997.
- [17] Dickson C. Heart Rate Artifact Suppression. Grand Valley State University. Masters Theses, Paper 18, 2012.
- [18] Li X., Chen J., Zhao G., Pietikainen M. Remote Heart Rate Measurement From Face Videos Under Realistic Situations. *IEEE*. 2014. doi: 10.1109/CVPR.2014.543
- [19] Poh M.-Z., McDuff D. J., Picard R. W. Advancements in Noncontact, Multiparameter Physiological Measurements Using a Webcam. *IEEE*. 58(1), 2011.

- [20] Akshay Asthana, Stefanos Zafeiriou, Shiyang Cheng, Maja Pantic, Robust Discriminative Response Map Fitting with Constrained Local Models, 2013 IEEE Conference on Computer Vision and Pattern Recognition.
- [21] Tomasi C., Kanade T. Detection and Tracking of Point Features. International Journal of Computer Vision. 1991.
- [22] Mellado I. Measuring heart rate with a smartphone camera. 2013 Sep 10 [cited 2014 April 11]. Available from: <http://www.ignaciomellado.es/blog/Measuring-heart-rate-with-a-smartphone-camera>.
- [23] Gibert G., D'Alessandro D., Lance F. Face detection method based on photoplethysmography. IEEE. 449-453, 2013. doi: 10.1109/AVSS.2013.6636681
- [24] Shannon C. E. Communication in the Presence of Noise. Proceedings of the IEEE. 86(2):447-457, 2002. doi: 10.1109/JPROC.1998.659497
- [25] Poh M.-Z., McDuff D. J., Picard R. W. Non-contact, automated cardiac pulse measurements using video imaging and blind source separation. Optical Society of America. 2010.
- [26] Boas D., Franceschini M. A. Near infrared imaging. Scholarpedia, 4(4):6997. 2009. doi:10.4249/scholarpedia.6997
- [27] Bakker A., Smith B., Ainslie P., Smith K. Applied Aspects of Ultrasonography in Humans. InTech. Chapter 3, 2012 April 25. doi: 10.5772/32493
- [28] Mengelkoch L. J., Martin D., Lawler J. A Review of the Principles of Pulse Oximetry and Accuracy of Pulse Oximeter Estimates during Exercise. PHYS THER. 74:40-49, 1994.
- [29] Scully C. G., Lee J., Meyer J., Gorbach A. M., Granquist-Fraser D., Mendelson Y., Chon K.H. Physiological Parameter Monitoring from Optical Recordings with a

- Mobile Phone. IEEE TRANSACTIONS ON BIOMEDICAL ENGINEERING. 59(2)
, 2012.
- [30] Kwon S., Lee J., Chung G. S., Park K. S. Validation of heart rate extraction through an iPhone accelerometer. IEEE. 2011. doi: 10.1109/IEMBS.2011.6091301
- [31] Lamonaca F., Kurylyak Y., Grimaldi D., Spagnuolo V. Reliable Pulse Rate Evaluation by Smartphone, IEEE International Symposium on Medical Measurements and Applications Proceedings (MeMeA), 1-4, 2012.
- [32] Pavlidis I., Dowdall J., Sun N., Puri C., Fei J., Garbey M. Interacting with human physiology, Computer Vision and Image Understanding. 108(1-2):150-170, 2007.
- [33] Takano C., Ohta Y. Heart rate measurement based on a time-lapse image. Med. Eng. Phys. 29(8):853-857, 2007.
- [34] Jonathan E., Martin L. Investigating a smartphone imaging unit for Photoplethysmography. Physiological Meas. 31(11):N79, 2010.
- [35] James C. J., Hesse C. W. Independent component analysis for biomedical signals. Physiol. Meas. 26(1): R15-R39, 2005.
- [36] Gregoski M. J., Mueller M., Vertegel A., Shaporev A., Jackson B. B., Frenzel R. M., Sprehn S. M., Treiber F. A. Development and Validation of a Smartphone Heart Rate Acquisition Application for Health Promotion and Wellness Telehealth Applications. Hindawi Publishing Corporation International Journal of Telemedicine and Applications. 2012. doi:10.1155/2012/696324
- [37] Vision.CascadeObjectDetector System object. Matlab. 2015. [cited 2015 April 11]
Available from:
<http://www.mathworks.com/help/vision/ref/vision.cascadeobjectdetector-class.html>

[38] Viola P., Jones M., Rapid object detection using a boosted cascade of simple features, IEEE. 2001.

[39] Technology. SkinFirst. [cited 2015 May 3] Available from:

<http://www.skinfirst.co.uk/treatments/technology/>

[40] Signal Processing ToolBox User's Guide R2014b. Matlab [cited 2015 May 3]

Available from: www.mathworks.com/help/pdf_doc/signal/signal_tb.pdf

Biographical Information

Negar Ziaee Nasrabadi received her Bachelor of Science in Computer Science from BIHE university, Tehran, Iran, in July 2010. She worked for Arish Afzar Asia an Electronic Corporation for more than two years in the Research and Development team. In this company she was working on a meter reader device that read the different meter data, prepared the data in a specific format and sent them through GPRS. The program was written for microcontroller. In fall 2013, she started her Master of Science in Computer Science in University of Texas at Arlington. Her research interest is intelligent system algorithm, machine learning, and software engineering.